THERMOLUMINESCENCE ASSESSMENT OF EU^{3+} AND DY^{3+} ION ACTIVATED $BA_2WO_3F_4$ PHOSPHORS IRRADIATED WITH Γ-PHOTON AND C^{5+} ION BEAM

K.V.Dabre [a*] and S.J. Dhoble[b]
[a]Deptartment of Physics, Arts, Commerce & Science College, Koradi, Nagpur-441111, India.
[b]Inter-University Accelerator Centre, Aruna Asaf Ali Marg, New Delhi, India.
[c]Department of Physics, R.T.M. Nagpur University, Nagpur-440033, India.

A B S T R A C T

Present work discusses about the synthesis and study of TL properties of Eu^{3+} and Dy^{3+} activated $Ba_2WO_3F_4$ phosphor irradiated with γ-photon and C^{5+} ion beam. The phosphor was synthesized by combination of wet chemical and solid state method. The as prepared phosphors are characterized by X-ray diffraction (XRD) for its phase purity, scanning electron microscope (SEM) for its microstructure and Thermoluminescence (TL) upon the irradiation of γ-photon and C^{5+} ion beam. XRD and SEM characterization reveals the formation of phase pure microcrystalline phosphor samples. TL response of both pure and rare earth activated phosphors was studied upon the γ-ray from ^{60}Co source and 75MeVC^{5+} ion beam irradiation. Effect of doping concentrations on TL response and dose response of the phosphor also studied. The glow curve of γ-ray irradiated samples shows the two glow peaks with intense one is at low temperature, whereas C^{5+} ion beam irradiated samples shows entirely different TL response. TL analysis and trapping parameters also determined in this work.

***Keywords:*Fluorotungstate,Thermoluminescence,γ irradiation,C^{5+} ion beam irradiation,Eu^{3+}/Dy^{3+}dopping**

1. Introduction

Oxy-fluorides have emerged as a new class of materials with interesting photoluminescent properties. Many of oxy-fluoride phosphor shows interesting luminescence properties and found to be promising candidate for the application in various field of luminescence **[1,2]**. In fact, the doping of oxygen in the fluoride glass such as BeF_2, AlF_3 etc. provides stability to the glasss system with improvement in optical properties because the M-O bond is less ionic than M-F bond and F^- ion is highly susceptible to hydrolysis **[2-5]**. Although oxide tungstates and molybdates are well known phosphors, luminescent behavior was not reported for oxy-fluoride tungstates until $Ba_2WO_3F_4$ was reported to be an efficient phosphor by Blasse et al. in 1984 **[1]**. As Blasse was astonished on high luminescence efficiency of $Ba_2WO_3F_4$ as $BaWO_4$ show weak luminescence even down to the liquid helium temperature; the luminescence investigation was also carried out for isostructuralmolybdate, $Ba_2MoO_3F_4$**[6]**, but it shows luminesces at low temperatures, due to the higher thermal quenching related to the size of the Mo^{6+} cation, which is the reason that the luminescence properties of tungstate based phosphor is more studied than molybdate based phosphor. The structural study of $Ba_2WO_3F_4$ was carried out by Wingefeldet. al**[7]** and Toradi et. al**[8]** and Blasse**[1]** has investigated it's the luminescence properties. All the while oxy-fluoride materials provide a unique host lattice for rare earth ions doping **[2,9,10]**. To the best of my knowledge after this no report on barium fluorotungstate is present in the literature. High luminescence efficiency of $Ba_2WO_3F_4$ makes my interest to investigate the luminescence properties when activated with rare earth.

Thermoluminescence (TL) is an extensive technique used for dosimetry of ionizing radiations as in this process, the intensity of light emitted by the phosphor on stimulation i.e. heating reflects the irradiation dose **[11-15]**. Thermoluminescent materials display,

deviations in dose response between sparsely ionizing radiation (high energy photons like X-rays and γ -rays) and densely ionizing radiation like heavy charged particles (HCP). This is due to different spatial dose distribution **[16]**.

Heavy ion beams have been used for diagnostic and therapeutic purposes for a long time now. The application of radiotherapy (RT) is based on the fundamental principle of achieving precise dose localization in the target lesion while causing minimal damage to surrounding normal tissues. Energy deposition of carbon ion beams increases with penetration depth up to the sharp maximum at the end of their range, known as the Bragg peak. Because the original peak is too narrow and sharp to completely cover the target lesion, broadening of the narrow peak according to the size of the lesion is used in cancer treatment **[17,18]**. This result in carbon ion beams allowing a highly localised deposition of energy that can be utilized for increasing radiation doses to tumours while minimising irradiation to adjacent normal tissues. Nevertheless, the dose of these energetic ions needs to be measured with great precision and accuracy, especially when dealing with human beings. This has triggered investigations to use thermoluminescent dosimeters (TLDs) for dose verification in heavy ion irradiation. In this respects Numan Salah have investigated Carbon ions irradiation on nano and microcrystalline $CaSO_4$:Dy a well-known TL material **[18]**.

Thus, in this work, the synthesis and study of TL properties of Eu^{3+} and Dy^{3+} activated $Ba_2WO_3F_4$ phosphor irradiated with γ-photon and C^{5+} ion beam carried out in this paper

2. Experimental

The analytically pure barium nitrate [$Ba(NO_3)_2$], tungstic acid (H_2WO_4), sodium tungstate (Na_2WO_4), ammonium fluoride (NH_4F) and rare earth oxide (Eu_2O_3 and Dy_2O_3) was used without further purification for the synthesis of $Ba_2WO_3F_4$:Eu_x,Na_x. The typical chemical reaction is given as follows:

$$\mathbf{Ba(NO_3)_2 + H_2WO_4 + 4\ NH_4F \rightarrow Ba_2WO_3F_4 + 4\ NH_3 + 2\ NO_2 + 3\ H_2O}$$

In typical synthesis, H_2WO_4 was added in the beaker containing solution of H_2O (distilled) and NH_3 (25%) in 1:1 ratio; the solution become turbid as H_2WO_4 is insoluble in H_2O, but sparingly soluble in NH_3. Thus, the solution was continuously stirred with heating on hot plate nearly for 1 hour, until the solution became clear. Simultaneously, the solutions of $Ba(NO_3)_2$ and NH_4F in distilled H_2O were prepared in separate beakers. Then the solution of $Ba(NO_3)_2$ was added drop wise in the solution of H_2WO_4 and stirred for 1 hour. After this the solution of NH_4F was added drop wise in the reaction mixture and stirred for 1 hour and final solution was kept in hot air oven at 80^{o}C for drying. The dried precursor was then mildly crushed in mortar pestle and heat treated at 500^{o}C for 12 hour followed by slow cooling to the room temperature in the furnace. The reaction mixture was taken out and crushed thoroughly for 1 hour and finally fired at 800^{o}C for 12 hours and allowed to cool to room temperature inside the furnace by switching it off. The final powdered material was used as is for further characterizations

The XRD patterns were obtain at room temperature from PANalytical X'Pert Pro X-ray diffractometer with Cu K_α radiation (λ = 1.5406A^o) operating at 40 kV voltage and 30 mA current. The morphology of the sample surface is analyzed by micrograph of the sample which is recorded on scanning electron microscope (SEM) (JEOL/EO, JSM-6380) operating at the voltage of 10kV. The TL glow curve of γ-rays (Co^{60} source) irradiated phosphor samples (5mg) in the dose range of 10Gy-1kGy was recorded. The pelletized samples of approximately 0.5mm thickness and 1cm diameter irradiated with C^{5+} ion beam of 75MeV energy from the 16MV Tandem Van de-Graff type Electrostatic Pelletron Accelerator at the Inter University Accelerator Center (IUAC), New Delhi, India [**19**]. The pelletized samples were mounted on a copper target ladder. The ion beam was magnetically scanned on a 1cm^2 area on pallet surfaces, after the irradiation the sample surface was scratched and 5mg of samples were weighed for TL glow curve measurement. The glow curves (GC) of the phosphor material were recorded using Harshaw TLD reader (model 3500). The heating rate (5^o/sec) was kept constant during recording of every GC.

3.Results & Discussion

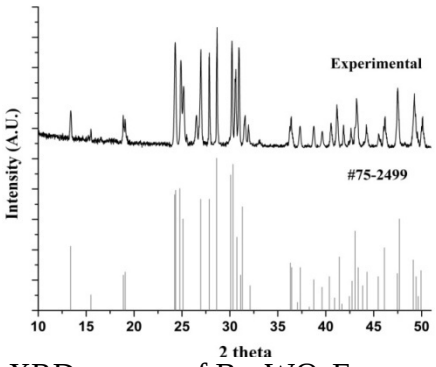

Fig. 1. XRD pattern of $Ba_2WO_3F_4$ compared with standard JCPDS file no. #75-2499.

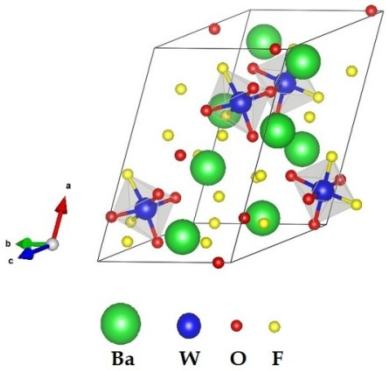

Fig. 2.Crystal structure of $Ba_2WO_3F_4$.

In order to evaluate the phase purity and crystalline state of the as synthesized undoped $Ba_2WO_3F_4$ phosphor sample the XRD pattern was recorded at room temperature and is illustrated in **Fig. 1**. The obtained XRD pattern reveals the formation of phase pure $Ba_2WO_3F_4$ phosphor crystallized in monoclinic phase with lattice parameter a = 11.51A^o, b = 9.398A^o, c = 7.197A^o, β = 126.11A^o and space group Cc (No. 9). The observed diffraction peaks are well consistent with standard JCPDS PDF #75-2499. The $Ba_2WO_3F_4$ has monoclinic structure contains chains of disordered WO_4F_2 octahedra with two F^- and two O^{2-} ions, both in cis position, which coordinate to one W^{6+} ion only. The individual octahedra share oxygen ions, giving a zig-zag chain with an O-W-O angle of 145^o [**6-8**]. In this zig-zag chain structure the Ba atom are placed alternatively with crystallographically two different sites both are at 4a site coordinated with different F^- and two 0^{2-} ions. The crystal structure of $Ba_2WO_3F_4$ is shown in **Fig. 2**.

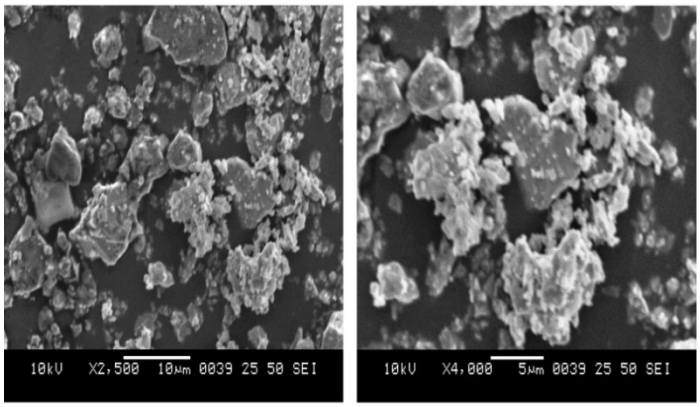

Fig. 3 SEM micrograph of as synthesized pure sample of $Ba_2WO_3F_4$ phosphor.

The microstructure and morphological properties of as synthesized pure sample of $Ba_2WO_3F_4$ phosphor was obtain at room temperature and is shown in **Fig. 3**. The typical micrograph of the samples shows the loose aggregate structure with varying size and shapes of the grains. The sizes of the grains are in the range from down to submicron (as can be seen from **Fig. 3b**)to 10 microns. The yield of grains of submicron to micrometer size could be realized by the synthesis route; as the initial reaction was carried out by wet chemical method for proper mixing and is responsible for submicron grains while the following prolong heating at high temperature leads to grain growth to micrometer size.

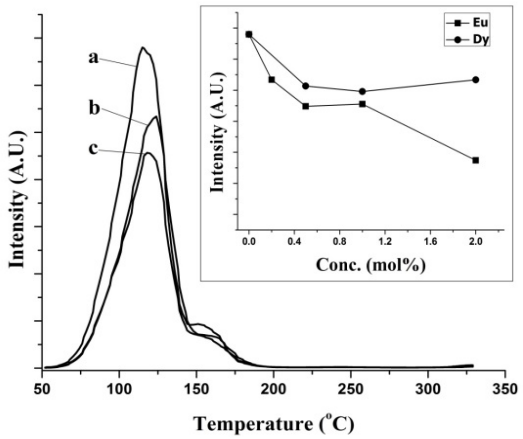

Fig. 4. TL glow curves of (a) $Ba_2WO_3F_4$, (b) $Ba_2WO_3F_4:Eu^{3+}$ (1mol%) and $Ba_2WO_3F_4$ (c) $Ba_2WO_3F_4:Dy^{3+}$ (2mol%) phosphor after irradiation by a gamma dose of1kGy from Co^{60} source. In inset, the variation of TL intensity of glow peak (~120°C) with activator concentration is presented.

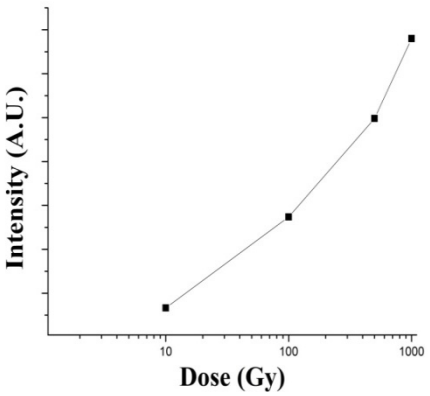

Fig. 5. Dose response curve of pure (glow peak at 115°C).

The TL properties of Eu^{3+} and Dy^{3+} ions doped $Ba_2WO_3F_4$ phosphors samples exposed to gamma radiation (Co^{60}) and C^{5+} ion beam are investigated. The TL glow curves of pure and rare earth (Eu^{3+}/Dy^{3+}) activated $Ba_2WO_3F_4$ phosphor irradiated with 1kGy of gamma dose from Co^{60} source is shown in Fig. 4. The glow curve of pure sample reveals two glow peaks; the intense one is at around 115°C and the small shoulder at around 160°C. The glow curve of Eu^{3+} and Dy^{3+} activated phosphor sample shows similar nature as that of pure sample with slight shifting of intense glow peak towards higher temperature (120°C for Eu^{3+} and 124°C for Dy^{3+}), while the intensity of weak shoulder peak at around 160°C seems to be unaffected with presence of dopant. Thus, it can be inferred that at least two types of defect center (traps) are results due to the gamma irradiation which are responsible for TL emission from both pure and rare earth activated phosphors. Out of these two defect center the defect center which is responsible for low temperature glow curve is sensitive to the presence of rare earth activator while the defect center which is responsible for the shoulder glow peak at 160°C is insensitive to the presence of rare earth activator

The intensity of low temperature glow peak has maximum intensity for pure sample and its intensity decreases with increase in both activators concentration as shown in inset of **Fig. 4**. The reduction in intensity with activator concentration might be the result of increase in non-radiative transition at activator center in the host lattice. The dose response of pure $Ba_2WO_3F_4$ phosphor is illustrated in **Fig. 5**. It is observed that the pure phosphor sample of $Ba_2WO_3F_4$ shows fairly linear response up to 500Gy of gamma dose and it became supralinear for subsequent higher dose.

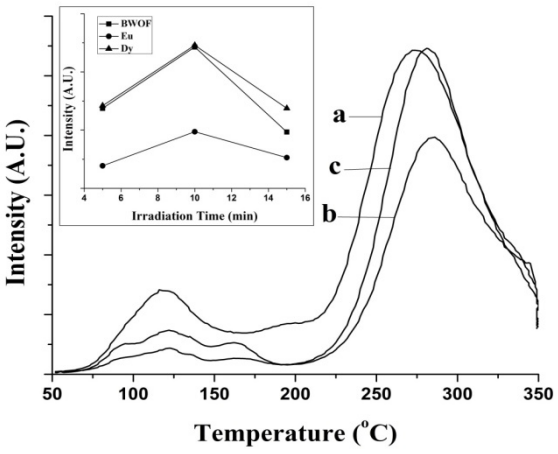

Fig. 6. TL glow curves of (a) $Ba_2WO_3F_4$, (b) $Ba_2WO_3F_4:Eu^{3+}$ (1mol%) and (c) $Ba_2WO_3F_4:Dy^{3+}$ (2mol%) phosphor after irradiation with a 75MeVC^{5+} ion beam from pelletron accelerator for 10min. In inset, the variation of TL intensity of glow peak (~280°C) with different irradiation time is presented.

The TL glow curve of the pure and Eu^{3+} and Dy^{3+} activated $Ba_2WO_3F_4$ phosphor upon irradiation with 75MeVC^{5+} ion beam from pelletron accelerator is shown in **Fig. 6.** The phosphor shows entirely different TL response to the carbon ion beam from γ-photon. The glow curve of both pure and Eu^{3+} and Dy^{3+} activated phosphor shows complex nature and consist of intense glow peak at around 280^{o}C and less intense glow peak at around 120^{o}C. This is conceivable that the conspicuous different TL response is due to the different types of ionizing radiations. Former is photon with comparatively less energy (1.17-1.33MeV) having zero rest mass and higher penetration power and later is ion beam with fairly large energy (75MeV) and less penetration power than gamma photon. Thus, it produces great number of surface defects in the material. As the ion beam irradiation facility was available for limited time the TL response of different concentration did not investigated.

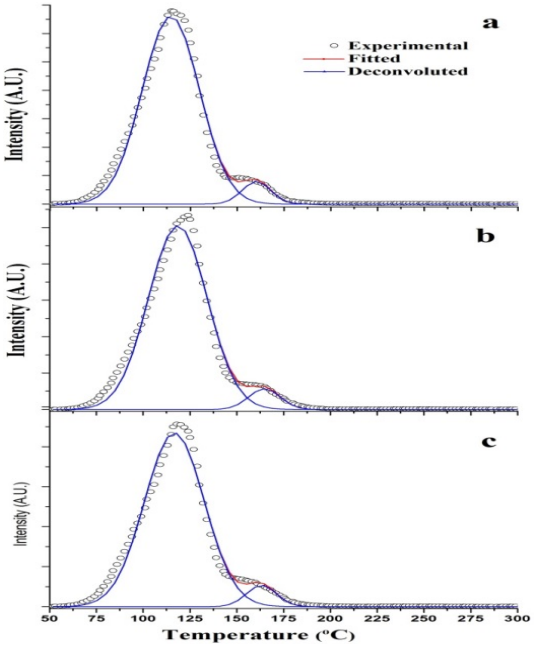

Fig. 7.TL glow curve deconvolution of (a) $Ba_2WO_3F_4$, (b) $Ba_2WO_3F_4$:Eu^{3+}, and (c) $Ba_2WO_3F_4$:Dy^{3+} phosphors upon the irradiation with γ-ray.

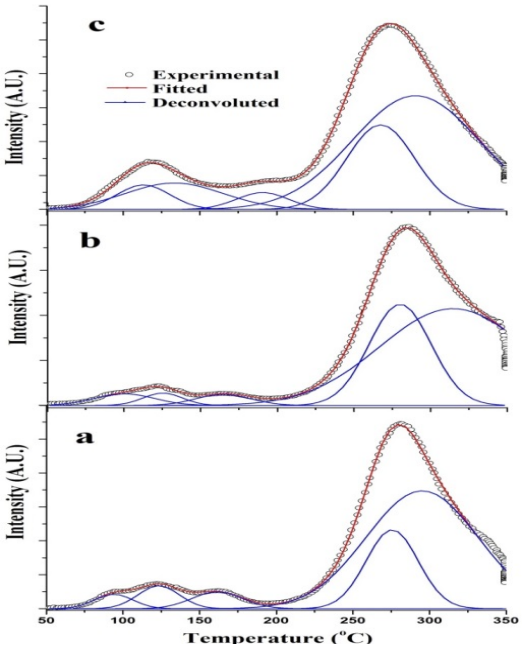

Fig. 8. TL glow curve deconvolution of (a) $Ba_2WO_3F_4$, (b) $Ba_2WO_3F_4$:Eu^{3+}, and (c) $Ba_2WO_3F_4$:Dy^{3+} phosphors upon the irradiation with C^{5+} ion beam.

It is observed that the intensity of glow curve of Eu^{3+} activated phosphor for all temperature is relatively lower than pure and Dy^{3+} activated phosphor. The intensity of high temperature glow peak of Dy^{3+} activated phosphor is same as that of pure phosphor sample, but the intensity of low temperature glow peaks is relatively lower than pure phosphor sample. The variation of intensity of high temperature glow curve at around 280^{o}C of the phosphors with different irradiation times are shown in inset of **Fig. 6.** It is seen that the intensity of glow peak increases with increase in irradiation time and the maximum intensity are observed for 10min of irradiation after which intensity decreases. The high temperature peak is less susceptible to fading thus it could be used as TLD phosphor to detect the dose up to 10min of irradiation. The decrease in intensity might be due to the degradation of the material by prolonging bombarding of ions; it is also worthwhile to note that the irradiated samples show no PL due to destruction of luminescence centre.

Kinetic (trapping) parameters determination has always been an active area of research for better understanding of the TL mechanism and important advances in TLD. Although a TL glow curve may look like a smooth continuum, it is actually composed of a number of overlapping peaks derived from the thermal release of electrons from traps of different stabilities. For this, to get the better understanding of various traps which results due to the irradiation of the phosphor sample to ionizing radiations, the computerized glow curve deconvolution method have been applied

and the kinetic parameters of each glow peak corresponding to one trap was calculated. **Fig. 7**and**8** shows the TL glow curve deconvolution of(a) $Ba_2WO_3F_4$, (b)$Ba_2WO_3F_4:Eu^{3+}$ and (c)$Ba_2WO_3F_4:Dy^{3+}$ phosphors upon the irradiation γ-ray and C^{5+} ion beam respectively. The Chen's glow curve peak shape method was applied to evaluate the kinetic parameters **[20]**.

To calculate trap parameters by peak shape method then peak shape parameter $\omega(=T_2-T_1)$, $\delta(=T_2-T_M)$ and $\tau(=T_M-T_1)$ are needed where T_1 and T_2 are the temperature at half maximum intensity at low and high temperature side respectively and T_M is temperature of maximum intensity. The order of kinetics can be predicted from shape of glow curve by using symmetry factor μ_g stated by Chen can be given as

,

$$\mu_g = \frac{\delta}{\omega} = \frac{T_2 - T_M}{T_2 - T_1} \text{ ---------- (1)}$$

Another symmetry factor to identify the order of kinetics proposed by Balarinγ can be given as,

$$\gamma = \frac{\delta}{\tau} = \frac{T_2 - T_M}{T_M - T_1} \text{ ---------- (2)}$$

The order of the kinetics (b) can be calculated from the graphical variation of order of kinetics with these two factors **[15]**. The activation energy and frequency factor is calculated by the formula which is given as follows:

$$E_\alpha = c_\alpha \left(\frac{kT_M^2}{\alpha} \right) - b_\alpha (2kT_M) \text{ ---------- (3)}$$

$$s = \frac{\beta E}{kT_M^2} \frac{e^{E/kT_M}}{(1+(b-1)2kT_M/E)} \text{ ---------- (4)}$$

Where, α stands for ω, τ and δ respectively and β is the heating rate (5^{o}C/sec). c_α and b_α can be given as,

$c_\tau = 1.51 + 3.0(\mu_g - 0.42)$ and $b_\tau = 1.58 + 4.2(\mu_g - 0.42)$

$c_\delta = 0.976 + 7.3(\mu_g - 0.42)$ and $b_\delta = 0$

$c_\omega = 2.52 + 10.2(\mu_g - 0.42)$ and $b_\omega = 0$

The evaluated trapping parameters of the phosphor irradiated with gamma photon and C^{5+} ion beam are compiled in **Table 1**and **2** respectively.

Table 1 Trap parameter of $Ba_2WO_3F_4$, $Ba_2WO_3F_4:Eu^{3+}$ and $Ba_2WO_3F_4:Dy^{3+}$ phosphor upon the irradiation with γ-ray.

Phosphor	Kinetic Parameters	Peak 1	Peak 2
$Ba_2WO_3F_4$	T_m (^{o}C)	113	160
	E (eV)	1.24	1.11
	s (sec^{-1})	9.53E15	2.09E12
$Ba_2WO_3F_4:Eu^{3+}$	T_m (^{o}C)	117	164
	E (eV)	1.27	1.114
	s (sec^{-1})	1.60E16	2.13E11
$Ba_2WO_3F_4:Dy^{3+}$	T_m (^{o}C)	117	164
	E (eV)	1.08	1..13
	s (sec^{-1})	4.92E13	4.66E13

Table 2Trap parameter of $Ba_2WO_3F_4$, $Ba_2WO_3F_4:Eu^{3+}$ and $Ba_2WO_3F_4:Dy^{3+}$ phosphor upon the irradiation with C^{5+} ion beam.

Phosphor	Kinetic Parameters	Peak 1	Peak 2	Peak 3	Peak 4	Peak 5
$Ba_2WO_3F_4$	T_m (^oC)	112	132	192	267	292
	E (eV)	1.00	1.27	1.32	1.59	0.81
	s (sec^{-1})	5.90 E12	2.534 E13	7.65 E13	2.56 E14	2.71 E7
$Ba_2WO_3F_4:Eu^{3+}$	T_m (^oC)	99	125	167	277	316
	E (eV)	0.81	1.32	0.95	1.76	--
	s (sec^{-1})	2.73 E10	2.52 E16	2.76 E10	4.79 E15	--
$Ba_2WO_3F_4:Dy^{3+}$	T_m (^oC)	92	122	163	274	294
	E (eV)	1.04	1.46	1.04	2.21	1.00
	s (sec^{-1})	1.89 E14	2.57 E17	4.31 E11	1.16 E20	1.76 E10

The activation energies of various traps corresponding to various glow peaks show slight variation whereas the frequency factor shows significant variation. Therefore, it is clear that there are some deep and shallow traps. The competition among them might be giving various releasing and retrapping probabilities, which might have resulted in different frequency factors. The traps could be either electron traps or hole traps or of both kind.

4.Conclusion

In summary, novel Eu^{3+} and Dy^{3+} activated barium fluorotungstate$Ba_2WO_3F_4$ phosphors are successfully synthesized by combination of wet chemical and solid state method. The XRD pattern of the sample reveals the formation of monoclinic phase of phosphor under study. The SEM micrograph of the sample shows the formation of the grains with irregular size and the dimensions ranging from submicron to few micrometers. The TL glow curve of the pure and Eu^{3+} and Dy^{3+} activated $Ba_2WO_3F_4$ phosphor irradiated with gamma photon shows two overlapped glow peaks; the intense one at low temperature around 120^oC and weak shoulder at moderate temperature around 160^oC. The sensitivity of pure phosphor is more than the doped phosphor. The pure phosphor shows linear response to 500Gy dose of gamma radiation and then the response became supralinear. The carbon ion beam irradiated sample exhibits complex glow curve having intense glow peak at higher temperature around 280^0 C which have highest intensity for 10min of irradiation. The calculated activation energies show slight variation due to the complex defect structures. For better understanding of the trapping centers in the phosphor material requires additional experimental results such as electron spin resonance (ESR).

REFERENCES

[1] Blasse, G., Verhaar, H.C.G., Lammers, M.J.J., Wingefeld, G., Hoppe, R., De Maayer, P., (1984). $Ba_2WO_3F_4$, A new fluorotungstate with high luminescence efficiency,*J. Lumin.* 29, 497-499.

[2] Sullivan, E., Vogt, T., (2013). Oxy-Fluoride Phosphors for Solid State Lighting, *ECS J. Solid State Sci. Tech.*, 2(2), R3088-R3099.

[3] Belsare, P.D., Joshi, C.P., Moharil, S.V., Kondawar, V.K., Muthalc, P.L., Dhopte, S.M., (2008). Luminescence of Eu^{2+} in some fluorides prepared by reactive atmosphere processing,*J. Alloys Compd.* 450, 468-472.

[4] Belsare, P.D., Moharil, S.V., Joshi, C.P., Omanwar, S.K., (2011). Preparation and Characterization of UV Emitting Fluoride Phosphors for Phototherapy Lamps, *AIP Conf. Proc.* 1391, 194-196.

[5] Belsare, P.D., Joshi, C.P., Moharil, S.V., Omanwar, S.K., Muthal, P.L., Dhopte, S.M., (2009). One step synthesis of Ce^{3+}

activated aluminofluoride powders,*Opt. Mater*. 31, 668-672.

[6] Wiegel, M., Blasse, G., (1993). Luminescence and nonlinear optical properties of bariumfluoromolybdate ($Ba_2MoO_3F_4$),*Solid State Comm.*, 86(4), 239-241.

[7] Wingefeld, G., Hoppe, R., (1984). *Z. anorg, allg. Chem.*, 518, 149.

[8] Torardi, C.C. &Brixner, L.H., (1985).Structure and luminescence of $Ba_2WO_3F_4$.*Mat. Res. Bul.*, 20, 137-145.

[9] Xia Z., Liu R.S., (2012). Tunable Blue-Green Color Emission and Energy Transfer of $Ca_2Al_3O_6F:Ce^{3+},Tb^{3+}$ Phosphors for Near-UV White LEDs.*J. Phys. Chem. C* 116, 15604-15609.

[10] Denault, K.A., George, N.C., Paden, S.R., Brinkley, S., Mikhailovsky, A.A., Neuefeind, J., DenBaarsab, S.P., Seshadri, R., (2012). A green-yellow emitting oxyfluoride solid solution phosphor $Sr_2Ba(AlO_4F)_{1-x}(SiO_5)_x:Ce^{3+}$ for thermally stable, high color rendition solid state white lighting.*J. Mater. Chem.*, 22, 18204-18213.

[11] Bos, A.J.J., (2007). Theory of thermoluminescence, *Radiat. Meas.* 41, S45-S56.

[12] Bos, A.J.J., (2001). On the energy conversion in thermoluminescence dosimetry materials,*Radiat. Meas.* 33, 737-744.

[13] Chen, R., Mckeever, S.W.S., *Theory of Thermoluminescence and Related Phenomenon*, (1997). World Scientific, London.

[14] Furetta, C., *Handbook of Thermoluminescence*, (2003). World Scientific, Singapore.

[15] Pagonis, V., Kitis, G., Furetta, C., *Numerical and Practical Exercises in Thermoluminescence*, (2006). Springer Science.

[16] Geiß, O.P, Krämer, M., & Kraft, G., (1998). *Nucl Instr & Meth B*, 142, 592-.

[17] Amaldi, U., Kraft, G., (2005). Radiotherapy with beams of carbon ions, *Rep. Prog. Phys.* 68, 1861-1882.

[18] Numan Salah, (2008). Carbon ions irradiation on nano and microcrystalline $CaSO_4$:Dy,*J. Phys. D: Appl. Phys.* 41, 155302.

[19] Kanjilal, D., Chopra, S., Narayanan, M.M., Iyer, I.S., Jha, V., Joshi, R., Datta, S.K., (1993). Testing and operation of the 15UD Pelleton at NSC, *Nucl. Instr. Methods Phys. Res. A* 328, 97-100.

[20] Chen, R., (1969). Glow Curves with General Order Kinetics, *J. Electrochem. Soc.* 116, 1254-1257.